A Two-Dimensional Zinc(II)–Schiff Base Coordination Polymer Formed by Six-Membered Metallacyclic Repeating Motif: Structural Aspects, Thermal and Photophysical Properties

Dipali Sadhukhan,[1] Aurkie Ray,[1] Georgina Rosair,[2] Loïc Charbonnière,[3] and Samiran Mitra*[1]

[1]Department of Chemistry, Jadavpur University, Raja S. C. Mullick Road, Kolkata 700032, West Bengal, India

[2]School of Engineering and Physical Sciences, Heriot Watt University, Edinburgh EH14 4AS, UK

[3]IPHC, UMR 7178 CNRS-UdS, ECPM, Bât R1N0, 25 rue Becquerel, 67087 Strasbourg Cedex 02, France

Received October 12, 2010; E-mail: smitra_2002@yahoo.com

A dicyanoamide-bridged 2D polynuclear zinc(II) complex having formula $[Zn_2(\mathbf{L})(\mu\text{-dca-}\kappa N^1\kappa N^5)_2]_n$, **1** has been synthesized using the Schiff base ligand *N*,*N*′-bis(salicylidene)-1,3-diaminopentane, ($\mathbf{H_2L}$) and sodium dicyanoamide [Na(dca)]. The complex presents a 2D hexagonal structure formed by 1,5-dca singly bridged helical chains connected through double 1,5-dca bridges. The ligand and the complex are well characterized by elemental analyses, IR and UV–vis spectroscopy. Thermogravimetric analysis is performed to investigate the thermal stability of the metal–organic framework. Photoluminescence studies of the Schiff base ligand in methanol and of the zinc(II) complex **1** in solid state show the presence of blue emission. The emission of the ligand occurs from an excited state involving an intramolecular proton-transfer process as a result of keto–enol tautomerisation and the zinc(II) complex emits from a ligand-centered excited state.

Design and synthesis of transition-metal coordination polymers are drawing attention of coordination chemists not only because of their interesting structural features as observed in the metal–organic frameworks or porous coordination polymers but also for their many possible applications in catalysis,[1] magnetism,[2] light emission, and electron-transport processes.[3]

Zinc plays an important role in biological systems being involved in cellular phenomena, e.g., enzyme catalysis,[4] apoptosis,[5] and neurotransmission.[6] In addition, electroluminescent (EL) zinc complexes are very promising systems for their interesting properties such as electron transport ability, light emitting efficiency, high thermal stability, ease of sublimation, and great diversity of tunable electronic properties resulting from ligand substitution.[7,8] In 1987 Tang and VanSlyke[9] reported $Al(q)_3$ (q: 8-hydroxyquinolinyl) as the first bilayer organic light-emitting diode (OLED). Since then, numerous attempts have been made in order to design green, blue, and red luminescent complexes to develop full color RGB devices as those three fundamental colors can be mixed to produce the whole visible spectrum. Interestingly, salicylaldehyde Schiff bases may play a role similar to that of 8-hydroxyquinoline for promoting photoluminescence in metal complexes since they have similar chromophoric groups i.e., a hydroxy group, a coordinating imine N atom and a delocalized π system.[10] Therefore, salen Schiff base complexes of zinc(II) are expected to show good luminescence properties. Luminescence properties of zinc(II) complexes originate from the organic ligand rather than LMCT because the d shell of the central ion is completely filled.[11] The metal plays a pivotal role in increasing the conformational rigidity and the extent of conjugation of the ligand, thus restricting energy loss via nonradiative decay such as vibrational motions and/or photo-induced electron transfer (PET)[12] leading to a bright and intense emission. In the case of Zn coordination polymers, the complex molecules are clipped into a very restricted metal organic framework, and are thus expected to gain extra conformational rigidity helpful for strong fluorescence intensity of the complex. As the Zn complexes based on salicylaldiminato Schiff base ligands emit in all the blue, greenish, and red region[13] and show good color purity there is a possibility to incorporate them in the list of electroluminescent complexes used for the fabrication of the full colored OLEDs.

In the present work we report the synthesis, X-ray crystal structure and physicochemical properties of a zinc(II) complex formulated as $[Zn_2(\mathbf{L})(\mu\text{-dca-}\kappa N^1\kappa N^5)_2]_n$, **1** formed with a N_2O_2 donor Schiff base ligand $\mathbf{H_2L}$ and dca as coligand. It represents a 2D coordination polymer formed by chiral helical chains connected through double dca bridges to form a hexagonal layer structure. The polymeric framework is thermally stable (up to 269 °C) and presents luminescence in the blue region.

Experimental

Syntheses. All solvents were of reagent grade and used without further purification. 1,3-Diaminopentane and salicylaldehyde were purchased from Aldrich Chemical Co. Sodium dicyanoamide was bought from Fluka. Zinc nitrate hexahydrate was purchased from E. Merck, India and was used as received.

Synthesis of the Schiff Base Ligand $OHC_6H_4CH{=}NCH_2CH_2CH(CH_2CH_3)N{=}CHC_6H_4OH$ [*N*,*N*′-Bis(salicylidene)-1,3-diaminopentane, ($\mathbf{H_2L}$)]. The Schiff base ligand ($\mathbf{H_2L}$) was prepared using a reported procedure (Scheme 1).[14]

Published on the web February 4, 2011; doi:10.1246/bcsj.20100290

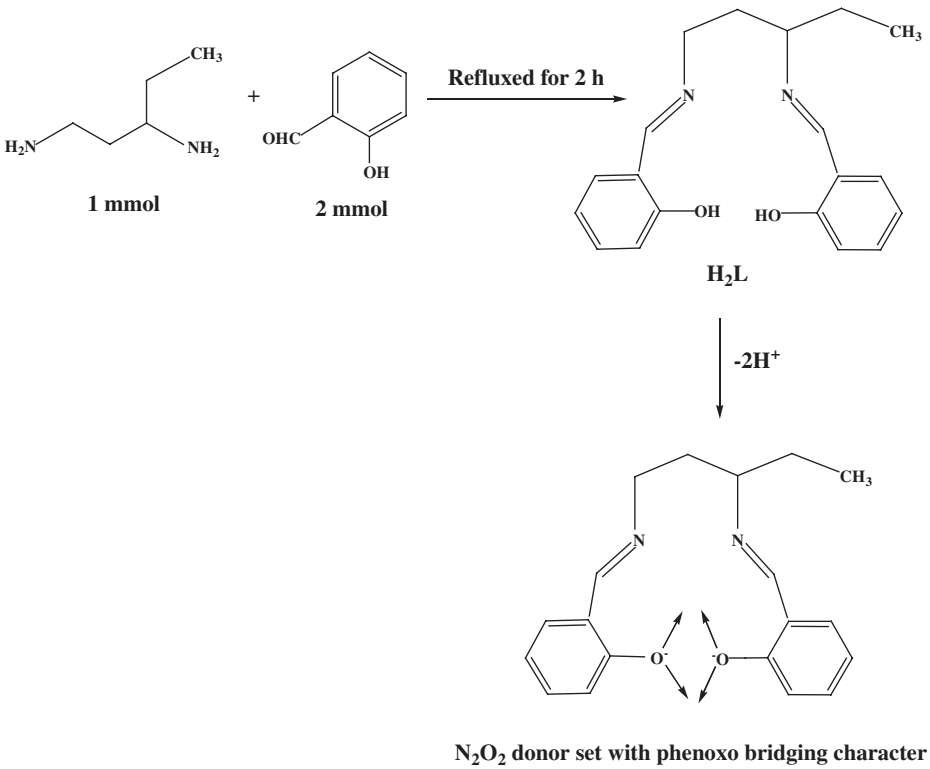

Scheme 1. Synthesis of the Schiff base $\mathbf{H_2L}$ and its coordination mode.

Elemental analysis: Found: C, 73.55; H, 7.0; N 9.03%. Calcd for $C_{19}H_{22}N_2O_2$: C, 73.52; H, 7.14; N, 9.03%. Main FT-IR bands (KBr, cm^{-1}): $\nu(C–O)_{phenolic}$ 1214, $\nu(C{=}N)$ 1631, $\nu(O–H)_{phenolic}$ 3537 cm^{-1}.

Synthesis of $[Zn_2(L)(\mu\text{-dca-}\kappa N^1\kappa N^5)_2]_n$, 1. **1** was prepared by mixing a solution of $Zn(NO_3)_2.6H_2O$ (0.446 g, 1.5 mmol) in 20 mL of methanol and 10 mL of a yellow methanolic solution of the Schiff base ($\mathbf{H_2L}$) (0.354 g, 1 mmol) under stirring. After addition of an aqueous solution of sodium dicyanoamide [Na(dca)] (0.133 g, 1.5 mmol) to this mixture, the resulting solution was allowed to stir for 15 min with gentle warming to avoid precipitation of the complex. The pale yellow solution was then filtered and kept at room temperature for crystallization by slow evaporation overnight to yield colorless needle shaped crystals suitable for X-ray crystallography. Crystals were isolated by filtration and were air-dried. Yield: 0.370 g (83%). Elemental analysis: Found: C, 48.32; H, 3.50; N, 19.61%. Calcd for $C_{23}H_{20}Zn_2N_8O_2$: C, 48.36; H, 3.53; N, 19.62%. Main FT-IR bands (KBr, cm^{-1}): $\nu(C–O)_{phenolic}$ 1151, $\nu(C{=}N)$ 1617, $\nu(C{\equiv}N)_{dca}$ 2160–2380 cm^{-1}.

Physical Measurements. Fourier transform infrared spectra were recorded in the range 4000–400 cm^{-1} on a Perkin-Elmer RX I FT-IR spectrophotometer with solid KBr pellets. The electronic spectra were recorded at 300 K on a Perkin-Elmer Lambda 40 (UV–vis) spectrometer with diffuse reflectance using paraffin oil matrix in a 1 cm quartz cuvette in the range 800–200 nm. C, H, and N microanalyses were carried out with a Perkin-Elmer 2400 II elemental analyzer. Fluorescence spectra were recorded on a Perkin-Elmer LS50B spectrometer equipped with a Xe flash lamp and using 1 cm^2 Suprasil quartz cells for liquid samples (Ligand) or 0.2 mm inner diameter quartz tube for solid samples of **1**. Excitation and emission spectra were corrected for the wavelength dependence of the lamp and PMT (Hamamatsu R928) using correction functions furnished by the manufacturer. Luminescence quantum yields, ϕ, were determined according to literature procedure,[15] using eq 1

$$\phi_x = \phi_{ref} \times \frac{\int I_{emx}(\lambda)d\lambda}{\int I_{emref}(\lambda)d\lambda} \times \left(\frac{n}{n_{ref}}\right)^2 \times \left(\frac{A_{ref}(\lambda_{exc})}{A_x(\lambda_{exc})}\right) \quad (1)$$

in which the subscripts x and ref refer to the sample and the reference respectively, $I_{em}(\lambda)$ is the corrected fluorescence spectrum, n is the refractive index of the medium and $A(\lambda_{exc})$ is the absorbance of the sample at the excitation wavelength. The reference compound used is rhodamine 6G in MeOH ($\varphi = 86\%$),[16] using optically diluted samples (d.o. <0.1). Thermogravimetric analysis of **1** was done in a Mettler Toledo TGA/SDTA 851 thermal analyzer.

X-ray Crystallography. The X-ray diffraction study of **1** was carried out at 100(2) K on a colorless needle shaped single crystal ($0.44 \times 0.22 \times 0.12$ mm^3). The crystal was mounted on a Bruker APEX-II CCD diffractometer with Mo Kα radiation ($\lambda = 0.71073$ Å). The lattice constants were refined by least-square refinement using 39573 total reflections ($2.68 < \theta < 26.41°$), 4858 unique reflections ($R_{int} = 0.0498$). Structure solution and refinement based on 4858 observed reflections with $I > 2\sigma(I)$ and 337 parameters gave final $R = 0.0488$, $wR = 0.0920$ with goodness-of-fit 1.126. Data collection and data reduction were done with the APEX 2 and SAINT programs respectively.[17,18] The structure was solved by direct methods by using the SHELXS-97 program and refined by full-matrix least-squares methods with the SHELXL-97 program.[19]

Table 1. Crystal Data for $[Zn_2(\mathbf{L})(\mu\text{-dca-}\kappa N^1\kappa N^5)_2]_n$ **1**

Empirical formula	$C_{23}H_{20}N_8O_2Zn_2$
Formula weight	571.21
Temperature	100(2) K
Wavelength	0.71073 Å
Crystal system	Monoclinic
Space group	$P2(1)/c$
a	9.7878(14) Å
b	12.1148(18) Å
c	20.178(3) Å
α	90°
β	91.426(5)°
γ	90°
Volume	2391.9(6) Å^3
Z	4
Density (calculated)	1.586 Mg m^{-3}
Absorption coefficient	2.043 mm^{-1}
$F(000)$	1160
Crystal size	0.44 × 0.22 × 0.12 mm^3
θ range for data collection	2.68 to 26.41°
Index ranges	$-12 \leqq h \leqq 12$
	$-15 \leqq k \leqq 15$
	$-25 \leqq l \leqq 25$
Reflections collected	39573
Independent reflections	4858 [R(int) = 0.0498]
Completeness to theta = 74.02°	99.2%
Absorption correction	Semiempirical
Max. and min. transmission	0.7916 and 0.6602
Refinement method	Full-matrix least-squares on F^2
Data/restraints/parameters	4858/13/337
Goodness-of-fit on F^2	1.126
Final R indices [$I > 2\sigma(I)$]	$R = 0.0488$, $wR = 0.0920$
R indices (all data)	$R = 0.0655$, $wR = 0.0975$
Largest diff. peak and hole	0.758 and −1.305 e.Å^{-3}

All non-hydrogen atoms were refined anisotropically by full-matrix least-squares based on F^2. The H atoms were generated geometrically and were included in the refinement in the riding model approximation. Selected crystallographic data, experimental conditions, and relevant features of the structural refinements for the complex are summarized in Table 1.

Crystallographic data have been deposited with Cambridge Crystallographic Data Centre: Deposition number CCDC-754867 for **1**. Copies of the data can be obtained free of charge via http://www.ccdc.cam.ac.uk/conts/retrieving.html (or from the Cambridge Crystallographic Data Centre, 12, Union Road, Cambridge, CB2 1EZ, U.K.; Fax: +44 1223 336033; e-mail: deposit@ccdc.cam.ac.uk).

Results and Discussion

Fourier Transform IR Spectra. The IR spectrum of **1** was analyzed and compared with that of the free ligand $\mathbf{H_2L}$ in the region 4000–400 cm^{-1}. A strong sharp absorption band around 1631 cm^{-1} in the spectrum of the Schiff base ligand can be assigned to the C=N stretching. Upon complexation with zinc, this band is shifted to 1617 cm^{-1} in **1** as a result of the coordination of the imine nitrogen to the metal center.[20–22] The ligand showed a well defined band at 3537 cm^{-1} due to O–H stretching which disappeared in the complex, indicating the deprotonation of the Schiff base ligand upon complexation. The strong phenolic C–O absorption band at 1214 cm^{-1} observed in the spectrum of the protonated free ligand, $\mathbf{H_2L}$, is shifted to 1151 cm^{-1} in **1**, supporting the deprotonation and the coordination of the phenolic oxygen atoms to the metal center, as confirmed by the structure of the complex.[22] **1** showed sharp absorption bands in the region 2160–2380 cm^{-1} evidencing the presence of dca ligand. The dicyanoamide anion in $NaN(CN)_2$ showed three sharp and strong characteristic bands in the frequency region 2290–2170 cm^{-1} which are attributed to $\nu_{as} + \nu_s(C{\equiv}N)$ combination modes (2286 cm^{-1}), $\nu_{as}(C{\equiv}N)$ (2232 cm^{-1}), and $\nu_s(C{\equiv}N)$ (2179 cm^{-1}).[23] In the complex these bands shift toward higher frequencies along with further splitting. In **1** those bands were found at 2370 (m) cm^{-1} ($\nu_{as} + \nu_s(C{\equiv}N)$); 2345 (m), 2323 (m) cm^{-1} ($\nu_{as}(C{\equiv}N)$), and 2253 (m), 2190 (s) cm^{-1} ($\nu_s(C{\equiv}N)$). These splitting and displacements of the bands toward higher frequencies clearly show the bidentate bridging mode of dca ligand[24] in **1** as evidenced by the X-ray crystal structure. The ligand coordination to the metal center is further substantiated by a band appearing at 461 cm^{-1} in **1** which is mainly attributed to ν_{Zn-N} in the complex.

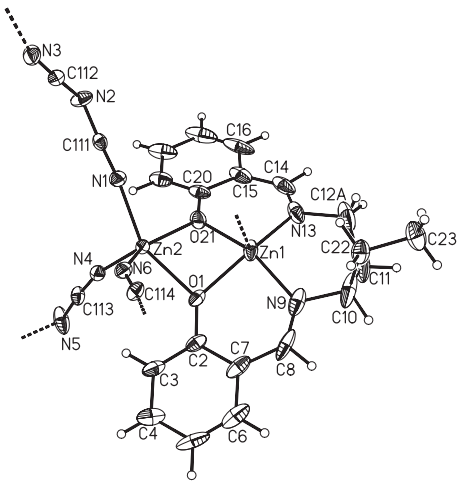

Figure 1. Perspective view of the asymmetric unit of **1** with displacement ellipsoids drawn at the 50% probability level.

Crystal Structure of $[Zn_2(\mathbf{L})(\mu\text{-dca-}\kappa N^1\kappa N^5)_2]_n$, 1. The asymmetric unit of the complex $[Zn_2(\mathbf{L})(\mu\text{-dca-}\kappa N^1\kappa N^5)_2]_n$, **1** is shown in Figure 1 and the bond distances and bond angles around the metal centers are listed in Tables 2 and 3 respectively. The asymmetric unit of **1** contains two dipositive metal ions (Zn1 and Zn2), a Schiff base ligand connecting both metal ions through a double phenolato bridge and two independent dca anions that connect each zinc(II) dimer with its three closest neighbors.

The dimetallic core consists of two five coordinate zinc(II) centers, Zn1 and Zn2 linked by the phenolato O atoms (O1 and O21) of the Schiff base. The Zn1–Zn2 separation is 3.0725(7) Å and is consistent with the reported Zn···Zn separation in double phenolato-bridged Zn complexes.[25,26] The Zn1 center enclosed by the Schiff base is closest to square-pyramidal geometry as defined by the Addison parameter $\tau = 0.2$ (Zn1) [$\tau = |\beta - \alpha|/60°$ where β and α are the two largest angles around the central atom; $\tau = 0$ and 1 for perfect

Table 2. Selected Bond Distances (Å) for **1**

Zn1–O21	2.044(3)
Zn1–N9	2.029(5)
Zn1–O1	2.044(3)
Zn1–N13	2.066(5)
Zn1–N3[a)]	2.058(4)
Zn1–Zn2	3.0725(7)
Zn2–N1	2.074(3)
Zn2–N4	1.986(4)
Zn2–N6[b)]	2.056(4)
Zn2–O1	2.126(3)
Zn2–O21	2.028(3)

a) Symmetry transformation: $-x+1, \quad -y+1, \quad -z+1$.
b) Symmetry transformation: $-x+1, y-1/2, -z+3/2$.

Table 3. Selected Bond Angles (°) for **1**

O21–Zn1–N9	158.70(15)
O21–Zn1–O1	74.35(11)
N9–Zn1–O1	90.23(16)
O21–Zn1–N13	88.46(18)
N9–Zn1–N13	97.2(2)
O1–Zn1–N13	146.61(16)
O21–Zn1–N3[a)]	95.11(14)
N9–Zn1–N3[a)]	101.95(16)
O1–Zn1–N3[a)]	99.35(13)
N13–Zn1–N3[a)]	110.71(16)
N1–Zn2–N4	105.08(14)
N1–Zn2–O1	150.40(13)
N4–Zn2–O1	103.76(13)
N1–Zn2–O21	90.13(13)
N4–Zn2–O21	112.00(13)
O1–Zn2–O21	72.94(12)
N1–Zn2–N6[b)]	91.35(14)
N4–Zn2–N6[b)]	107.48(14)
O1–Zn2–N6[b)]	86.26(13)
O21–Zn2–N6[b)]	138.61(14)

a) Symmetry transformation: $-x+1, \quad -y+1, \quad -z+1$.
b) Symmetry transformation: $-x+1, y-1/2, -z+3/2$.

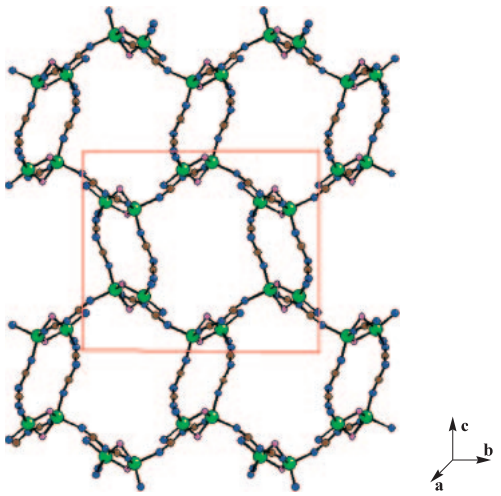

Figure 2. A hexagonal 2D metallacyclic pore made by the phenolato-bridged dimeric zinc(II) core connected by dca bridges in **1** (enclosed within the red square).

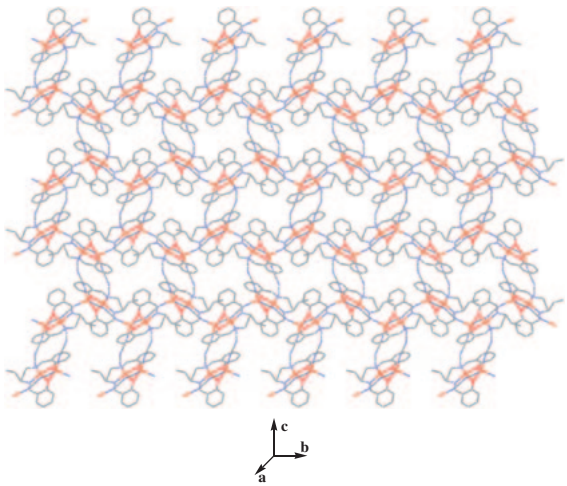

Figure 3. Polymeric view of **1** along the crystallographic *a* axis.

square-pyramidal and trigonal-bipyramidal geometries, respectively].[27] The dca bridge is in the axial position of Zn1 and binds to Zn2. The second metal center (Zn2) is also square pyramidal with $\tau = 0.26$. Two phenolato O atoms (O1 and O21) and three dca N atoms (N1, N4, and N6) complete the five coordinate coordination sphere. One of these dca bridges binds to Zn1 to give a doubly bridged centrosymmetric dimer. Using the four metal centers to define a parallelogram for **1** the acute Zn–Zn–Zn angle is 65.08°. The other two dca bridges on Zn2 bind to two symmetry equivalent neighboring Zn1 centers, both related by the screw axis along the *b* axis. The links to these neighboring molecules are single bridges. The single dca bridges from Zn2 to symmetry equivalent centers form six-membered rings (counting each dimetallic core as one node) resulting in a metallacyclic pore shown in Figure 2. These six-membered rings extend in two dimensions giving an undulating sheet in the 010 plane. Between the undulating sheets the benzene rings in the Schiff base interdigitate but in **1** the centroid to centroid distance exceeds 3.9 Å which is too long for π–π interactions (Figure 3).

All dca ligands are bridging in the $\mu_{1,5}$ mode. This is also the case in the binuclear Schiff base species $[Zn_2(salpn)(\mu\text{-dca-}\kappa N^1\kappa N^5)_2]_n$ and $[CdCu(salpn)(\mu\text{-dca-}\kappa N^1\kappa N^5)_2]_n$ where salpn: bis(salicylidene)-1,3-diiminopropanato.[28] These two complexes also form undulating sheets albeit with different motifs. Four bimetallic cores are bridged to form a metallacyclic pore whereas in **1** six bimetallic cores form this pore. The distinct difference in motif formation between **1** and the previously reported complexes lies within the ligand design. The amine used to synthesize $\mathbf{H_2L}$ is 1,3-diaminopentane whereas 1,3-diaminopropane was used to synthesize salpn. The well known steric effect of the bulky ethyl group attached to C10 in **1** prevents association of four bimetallic cores within a metallacycle bridged by dca, rather formation of a six-membered metallacyclic repeating unit is the optimum requirement for this particular ligand system $\mathbf{H_2L}$. Moreover the packing features of **1** (Figure 3) show that it is a single-layered sheet-like

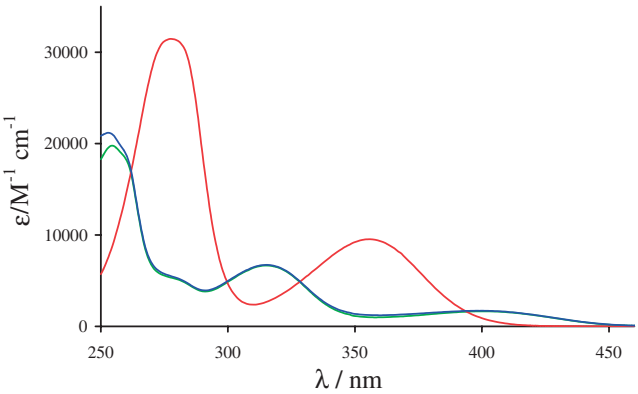

Figure 4. UV–vis absorption spectra of $\mathbf{H_2L}$ (2 mL, 6.45×10^{-5} M) in MeOH (green), and upon addition of 10 μL Et_3N (blue) or of 10 μL conc. HCl (red).

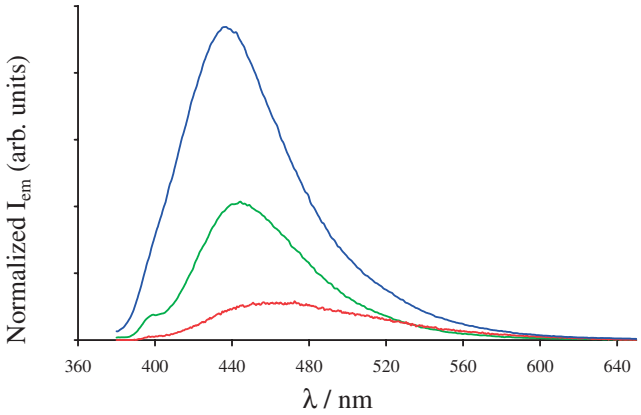

Figure 5. Normalized emission spectra of $\mathbf{H_2L}$ in MeOH (green), and in the presence of Et_3N (blue) or of conc. HCl (red). All spectra are obtained upon excitation at 357 nm, and surface normalized according to their luminescence quantum yield (see text).

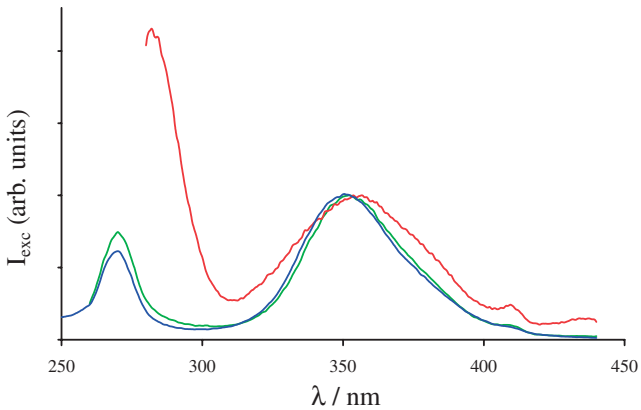

Figure 6. Normalized excitation spectra of $\mathbf{H_2L}$ in MeOH (green) and in the presence of Et_3N (blue) or conc. HCl (red). All spectra are normalized on the maximum of the low energy excitation band ($\lambda_{em} = 465$ nm).

polymeric network constituted of consecutive right-handed and left-handed horizontal helices vertically interconnected, distinctly different from the steps like architecture formed of square grids in case of the above-mentioned salpn complexes.

Photophysical Studies on $[Zn_2(L)(\mu\text{-dca-}\kappa N^1\kappa N^5)_2]_n$, 1 and $\mathbf{H_2L}$. UV–vis Absorption Spectra: UV–vis spectra of the free ligand and the complex were recorded at 300 K by diffuse reflectance in paraffin oil matrix. The UV–vis spectrum of the Schiff base ligand $\mathbf{H_2L}$ exhibited two absorption bands at 255 and 308 nm which can be attributed to $\pi \rightarrow \pi^*$ and $n \rightarrow \pi^*$ transitions within the Schiff base ligand. Three distinct absorption bands appeared in the spectra of the complex, **1** at 213, 331, and 380 nm. The ligand-centered absorption bands of $\mathbf{H_2L}$ at 255 and 308 nm may have suffered large bathochromic shifts in the spectrum of the complex appearing at 331 and 380 nm in **1**. The band at 213 nm in **1** can be considered as a $L \rightarrow M$ charge-transfer transition since this band was not observed in the spectrum of the free ligand and occurs probably from the 2p orbital of phenolato oxygens to the empty 4s orbital of Zn^{2+} ion and requires high energy.[29]

Absorption and Emission of the Ligand $\mathbf{H_2L}$ in MeOH: In order to better understand the origin of the observed absorption bands and the resulting luminescence properties of compounds $\mathbf{H_2L}$ and **1**, the spectroscopic properties of the ligand were further studied in MeOH solutions. Figure 4 displays the UV–vis absorption spectrum of a solution of the ligand in MeOH. The spectrum is dominated by two intense absorption bands at 401 ($\varepsilon = 1720\ M^{-1}\ cm^{-1}$) and 314 nm ($\varepsilon = 5980\ M^{-1}\ cm^{-1}$). Both the shape and the intensity of the absorption spectrum are typical of bis(iminophenolato) ligands.[30]

The UV–vis absorption spectrum is almost unchanged in the presence of a base, but greatly influenced by the presence of hydrochloric acid into the solution. The absorption maxima is then hypsochromically shifted to 355 nm ($\varepsilon = 9500\ M^{-1}\ cm^{-1}$), corresponding to the energy level observed for salen type ligands complexed by metal atoms such as Zn.[10,31] Upon excitation into the UV domain, the emission spectrum displays a broad emission band with a maximum at 445 nm (Figure 5) and a luminescence quantum yield of 0.93%. Interestingly, while the addition of Et_3N has almost no impact on the absorption spectrum, it resulted in a nearly twofold increase of the luminescence quantum yield, which reached 2.2%, with a small hypsochromic shift of the emission maximum at 439 nm. In contrast, addition of HCl resulted in a large decrease of the luminescence efficiency, which dropped to 0.36%, and was bathochromically shifted to 464 nm.

In MeOH, both acidic and basic media, the excitation spectra are similar, with a maximum at ca. 353 nm (Figure 6). Surprisingly, but in accordance with previous observations[30] the excitation spectra of $\mathbf{H_2L}$ cannot be related to any observed transition in the absorption spectra of $\mathbf{H_2L}$ in MeOH or Et_3N, but the excitation spectra of $\mathbf{H_2L}$ in all neutral, acidic, and basic media can be well correlated to its absorption spectrum in acidic medium (Figures 4 and 6). Only in the case of the acidic solution it is possible to notice a broadening of the excitation band, together with a bathochromic shift of the low energy excitation band at 280 nm. The presence of the excitation maximum at this energy level is in agreement with the excitation spectra observed for europium complexes of salen.[32]

This behavior is surprising as the concordance of the excitation spectra and of the absorption spectrum in acidic

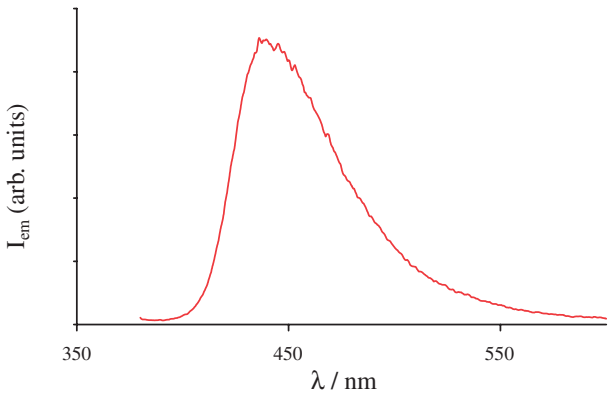

Figure 7. Emission spectrum of **1** in the solid state (rt, $\lambda_{exc} = 350$ nm).

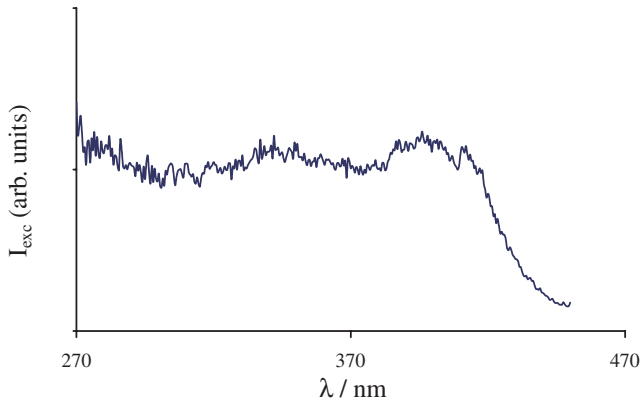

Figure 8. Excitation spectrum of **1** (solid state, rt, $\lambda_{em} =$ 520 nm).

conditions points to an emission arising from a protonated species of the ligand. Nevertheless, such behavior is typical of salicylaldehyde[33] and salicylideneaniline[34] derivatives. It is attributed to emission arising from a keto–enol tautomerism in the excited state, that can be observed in numerous ortho-substituted phenolic compounds for which a H-bond can be formed between the hydroxy function and the substituent in ortho position.[35]

Solid-State Luminescence Properties of 1: As evidenced in Figure 7, the zinc complex **1** in the solid state displayed an intense emission band with maximum at 440 nm, 5 nm hypsochromically shifted compared to the free ligand, but almost at the same energy level as $\mathbf{H_2L}$ in the presence of Et_3N. This luminescence is typical of zinc(II) Schiff base complexes.[36] A similar emission pattern was also recently observed in a Zn_2Tb_3 complex of salen, in which an incomplete energy transfer from the ligand to the Tb atom was observed, with admixture of emission arising from both the salen ligand and the Tb atom.[37] In the case of **1** the emission band is preferably attributed to the ligand-based transitions rather than LMCT as the d shell of the zinc(II) ion is completely filled.[8] Like any other salen Schiff bases, $\mathbf{H_2L}$ or $\mathbf{L^{2-}}$ are intrinsic fluorophores as they contain azomethine-conjugated aromatic nuclei.[8] It was shown previously[38] that on increasing the number of π conjugation as well as the iminophenolato moieties in a salen type Schiff base ligand backbone, the emission bands of the complexes are red-shifted. In other words the emission of salen type complexes are originally ligand based mainly originating from the iminophenolato chromophore. The role of the zinc ion is to impose conformational rigidity and the extent of conjugation of the ligand, thus restricting energy loss via nonradiative decay such as vibrational motions and/or photo-induced electron transfer (PET)[11,12] leading to a bright and intense emission.

The excitation spectrum of **1** is presented in Figure 8 and shows the excitation to be strong from 450 nm to the UV region, indicative of an excitation through the ligand-centered absorption bands. Unfortunately, saturation phenomena did not allow a precise determination of the excitation maximum in that case.

Upon imposition of a 20 μs delay time between excitation and integration of the emission intensity, the emission band totally vanished, pointing to a short excited state lifetime and to a singlet excited state centered on the ligand, arising from $\pi \rightarrow \pi^*$ and/or $n \rightarrow \pi^*$ singlet emission of the iminophenolato moieties.

Thermogravimetric Analysis. In order to use complexes as emissive materials it is important to look into their thermal stability. The thermal stability of **1** has been investigated using TGA over a temperature range 25–600 and 25–1200 °C in two consecutive runs in dynamic nitrogen atmosphere. The thermogram of the first run states that **1** is stable up to 269 °C. After that temperature a gradual mass loss occurs up to 492 °C. At this stage a 12.5% mass loss occurs which is due to decomposition of dca and is in good agreement with the calculated value (11.56%). The powder obtained after this run was investigated with FT-IR. The IR spectrum clearly shows the disappearance of dca peaks in the region 2190–2370 cm^{-1}, but the Schiff base stretching frequencies are still present i.e. the dca-bridged 2D network is stable up to 269 °C. In the second run in addition to dca mass loss another 63.2% mass loss occurs within the temperature range 654–937 °C which corresponds to the decomposition of $\mathbf{L^{2-}}$ (calculated value 65.08%) after which no further mass loss was observed.

Conclusion

This paper describes the synthesis and structural aspects of a dicyanoamide-bridged 2D polymeric zinc complex with a N_2O_2 donor Schiff base ligand and its applications in photophysical fields. The Schiff base on combination with zinc(II) produces an excellent blue luminescent species providing a ligand-centered singlet excited state to emit in the visible blue light region. Though most of the activities of the complex are due to the metal ion and the Schiff base ligand fragment the dicyanoamide linker also plays some crucial role to form a two-dimensional undulating sheet-like metal–organic framework and to impose thermal stability. Furthermore, the presence of vacant coordination sites on the square-planar-chelated zinc(II) atom and especially on the nonchelated zinc(II) ion offers up to 1 + 3 bridging points (if we assume pentacoordination for the zinc(II) ions). The addition of a highly potential bridging ligand as dca has led, as expected, to the formation of up to four dca bridges connecting the vacant positions of the zinc ions. This coordination mode generates a 2D coordination polymer

with helical –Zn–dca–Zn– chains that are further connected through double dca bridges to form a 2D layer with a repeating hexagonal metallacyclic motif.

We are thankful to University Grants Commission and Council of Scientific and Industrial Research, New Delhi, Government of India for financial help.

References

1 J. Y. Lee, O. K. Farha, J. Roberts, K. A. Scheidt, S. B. T. Nguyen, J. T. Hupp, *Chem. Soc. Rev.* **2009**, *38*, 1450.

2 M. Kurmoo, *Chem. Soc. Rev.* **2009**, *38*, 1353.

3 M. D. Allendorf, C. A. Bauer, R. K. Bhakta, R. J. T. Houk, *Chem. Soc. Rev.* **2009**, *38*, 1330.

4 S. J. Lippard, J. M. Berg, *Principles of Bioinorganic Chemistry*, University Science Books, Mill Valley, CA, USA, **1994**.

5 E. Kimura, S. Aoki, E. Kikuta, T. Koike, *Proc. Natl. Acad. Sci. U.S.A.* **2003**, *100*, 3731.

6 S. C. Burdette, S. J. Lippard, *Proc. Natl. Acad. Sci. U.S.A.* **2003**, *100*, 3605.

7 W. Yang, H. Schmider, Q. Wu, Y. Zhang, S. Wang, *Inorg. Chem.* **2000**, *39*, 2397.

8 J. He, Y.-G. Yin, X.-C. Huang, D. Li, *Inorg. Chem. Commun.* **2006**, *9*, 205.

9 C. W. Tang, S. A. VanSlyke, *Appl. Phys. Lett.* **1987**, *51*, 913.

10 T. Yu, W. Su, W. Li, Z. Hong, R. Hua, M. Li, B. Chu, B. Li, Z. Zhang, Z. Z. Hu, *Inorg. Chim. Acta* **2006**, *359*, 2246.

11 S. Basak, S. Sen, S. Banerjee, S. Mitra, G. Rosair, M. T. G. Rodriguez, *Polyhedron* **2007**, *26*, 5104.

12 A. Majumder, G. M. Rosair, A. Mallick, N. Chattopadhyay, S. Mitra, *Polyhedron* **2006**, *25*, 1753.

13 V. Liuzzo, W. Oberhauser, A. Pucci, *Inorg. Chem. Commun.* **2010**, *13*, 686.

14 A. Ray, D. Sadhukhan, G. M. Rosair, C. J. Gómez-García, S. Mitra, *Polyhedron* **2009**, *28*, 3542.

15 B. Valeur, *Molecular Fluorescence: Principles and Applications*, Wiley-VCH, Weinheim, **2002**, p. 161.

16 J. Olmsted, *J. Phys. Chem.* **1979**, *83*, 2581.

17 *APEX2 Version 2.1: Area Detector Control and Integration Software, v. 6.45*, Bruker Analytical X-ray Instruments, Inc., Madison, WI, USA, **2006**.

18 *Area-Detector Integration Software*, Siemens Industrial Automation, Inc., Madison, WI, **1995**.

19 G. M. Sheldrick, *SHELX-97*, University of Göttingen, **1997**.

20 M. Dolaz, M. Tümer, M. Diğrak, *Transition Met. Chem.* **2004**, *29*, 528.

21 K. Nakamoto, *Infrared and Raman Spectra of Inorganic and Coordination Compounds, Part A: Theory and Applications in Inorganic Chemistry*, 5th ed., John Willey & Sons Inc., New York, **1997**.

22 Z.-L. You, H.-L. Z. Zhu, *Z. Anorg. Allg. Chem.* **2004**, *630*, 2754.

23 A. Ray, G. Pilet, C. J. Gómez-García, S. Mitra, *Polyhedron* **2009**, *28*, 511.

24 B. Vangdal, J. Carranza, F. Lloret, M. Julve, J. Sletten, *J. Chem. Soc., Dalton Trans.* **2002**, 566.

25 J. S. Matalobos, A. M. García-Deibe, M. Fondo, D. Navarro, M. R. Bermejo, *Inorg. Chem. Commun.* **2004**, *7*, 311.

26 C. Maxim, T. D. Pasatoiu, V. Ch. Kravtsov, S. Shova, C. A. Muryn, R. E. P. Winpenny, F. Tuna, M. Andruh, *Inorg. Chim. Acta* **2008**, *361*, 3903.

27 A. W. Addison, T. N. Rao, J. Reedijk, J. van Rijn, G. C. Verschoor, *J. Chem. Soc., Dalton Trans.* **1984**, 1349.

28 Q. Shi, L. Sheng, K. Ma, Y. Sun, X. Cai, R. Liu, S. Wang, *Inorg. Chem. Commun.* **2009**, *12*, 255.

29 T. Tuerk, U. Resch, M. A. Fox, A. Vogler, *Inorg. Chem.* **1992**, *31*, 1854.

30 J. Chakraborty, S. Thakurta, G. Pilet, R. Z. Ziessel, L. J. Charbonnière, S. Mitra, *Eur. J. Inorg. Chem.* **2009**, 3993.

31 F. Gao, W.-J. Ruan, J.-M. Chen, Y.-H. Zhang, Z.-A. Zhu, *Spectrochim. Acta, Part A* **2005**, *62*, 886.

32 J. T. Mitchell-Koch, A. S. Borovik, *Chem. Mater.* **2003**, *15*, 3490.

33 L. Rodríguez-Santiago, M. Sodupe, A. Oliva, J. Bertran, *J. Am. Chem. Soc.* **1999**, *121*, 8882.

34 S. Mitra, N. Tamai, *Chem. Phys. Lett.* **1998**, *282*, 391.

35 J. Catalan, F. Toribio, A. U. Acuña, *J. Phys. Chem.* **1982**, *86*, 303.

36 C.-C. Kwok, S.-C. Yu, I. H. T. Sham, C.-M. Che, *Chem. Commun.* **2004**, 2758.

37 C. E. Burrow, T. J. Burchell, P.-H. Lin, F. Habib, W. Wernsdorfer, R. Clérac, M. Murugesu, *Inorg. Chem.* **2009**, *48*, 8051.

38 S. Mizukami, H. Houjou, Y. Nagawa, M. Kanesato, *Chem. Commun.* **2003**, 1148.